Korean J. Chem. Eng., 34(5), 1584-1590 (2017)
DOI: 10.1007/s11814-017-0003-7

pISSN: 0256-1115
eISSN: 1975-7220

Enhanced photoactivity of N-doped TiO_2 for Cr(VI) removal: Influencing factors and mechanism

Shu Qin Wang*,†, Wen Bo Liu*, Peng Fu, and Wei Liang Cheng*,†**

*School of Environmental Science and Engineering, North China Electric Power University, Baoding, Hebei 071003, P. R. China
**Sailhero Environmental Protection Hi-tech Co., Ltd., No. 251, Xiangjiang Road, Shijiazhuang City, Hebei, P. R. China
(*Received 4 September 2016 • accepted 2 January 2017*)

Abstract−To further enhance the photoactivity of virgin TiO_2, we prepared N-doped TiO_2 (N-TiO_2) by sol-gel method and used it to remove Cr(VI) ions from water under visible light. The catalysts were characterized by TEM, XRD, BET and UV-vis techniques. Better crystalline structure, larger specific surface area and decreased band-gap width were obtained after the insertion of N atoms into TiO_2 lattice. Several influencing factors were also investigated. The removal efficiency of Cr(VI) increases with the decrease of initial Cr(VI) concentration or the increase of catalyst dosage. Addition of glucose or some inorganic ions (Mg^{2+}, Al^{3+}) can promote the photoreduction process by improving the quantum efficiency. The kinetics and mechanism were discussed as well.

Keywords: Photocatalytic Reduction, Cr(VI), N-doped TiO_2, Influencing Factors, Kinetics, Mechanism

INTRODUCTION

With the development of energy systems, various types of clean energy configurations and fuel prototypes have induced massive investigations [1-4]. However, in the custom fossil fuel industry, chromium, especially hexavalent chromium, remains a highly toxic environmental pollutant that has carcinogenic, mutagenic and teratogenic effects on some specific organisms. In coal-fired power plants, Cr(VI) usually exists in the ash wastewater and results in water pollution. In addition, industrial parks, manufacturing, mining and ore processing, leather, industrial waste dumps, chemical manufacturing, and fuel industry also cause chromium pollution. Reduction method is a common method for Cr(VI) removal as the toxicity of Cr(III) is much less than that of Cr(VI) and can be easily precipitated as $Cr(OH)_3$ in neutral or alkaline solutions. However, the traditionally-used chemicals for Cr(VI) reduction suffer from high cost and secondary pollution.

In recent years, TiO_2 has become a research focus for the treatment of Cr(VI)-containing wastewater due to its strong photoactivity, high efficiency, chemical stability, no secondary pollution, low cost and nontoxicity [5-7]. Cr(VI) was firstly adsorbed onto the surface of TiO_2 and then reduced to Cr(III) by photoinduced electrons. However, because of the wide band gap, the treatment of Cr(VI) using TiO_2 was mostly studied under ultraviolet light [8-10]. Recent studies have shown that doping is an attractive option to improve the light absorption in visible region [11,12]. Hu et al. found that N doping can improve the light responding ability of TiO_2, thereby increasing the removal efficiency of Brilliant Blue KN-R to 80% [14].

Although there have been many intensive studies on photocatalytic phenomena [13-15], the details and mechanism of the photoreduction of Cr(VI) by TiO_2 have not been fully researched yet. Therefore, we have prepared N-doped TiO_2 via sol-gel method and used it to remove Cr(VI) ions from water under visible light. As the optimum preparation conditions have been discussed in our previous research [16], this work was mainly focused on the influencing factors of the photocatalytic process such as light irradiation, catalyst dosage, initial Cr(VI) concentration, coexisting of inorganic cations and addition of hole scavenger (glucose in this case). Further detailed discussions regarding the mechanism of photocatalytic reduction process under visible light were conducted as well.

EXPERIMENTAL

1. The Preparation of TiO_2

N-TiO_2 catalysts were synthesized according a sol-gel method reported in our previous research [16]. The process was briefly described as follows. Two different solutions (A and B) were prepared at first. 40 mL absolute ethyl alcohol, 0.5 g hexamethylenetetramine and 17 mL butyl titanate were mixed to form solution A. On the other hand, 40 mL absolute ethyl alcohol, 5 mL glacial acetic acid and 5 mL deionized water were mixed to form solution B. Both operations were under magnetic stirring. Next, solution A was slowly dripped into solution B with slow stirring to form a white gel, which was then sealed up and left standing for 24 hours. The resulting gel was dried by microwave and ground into powder. At last, these powders were calcined in a muffle furnace at 500 °C for 3 h to obtain the needed catalyst labeled as N-TiO_2. The virgin TiO_2 was prepared by the same method.

†To whom correspondence should be addressed.
E-mail: wsqhg@163.com, cheng_w_l@163.com, cheng_w_l@126.com
‡The paper will be reported in the 11th China-Korea Clean Energy Workshop.

2. Characterizations

Transmission electron microscopy (TEM) (XM 5136, Tescan, Czechia) was used to observe the sample particle size and morphology. The crystalline structures of virgin TiO_2 and N-TiO_2 were investigated using X-ray diffraction (XRD) technique (Y2000, Dandong, China). The specific surface area and pore distributions were determined by BET analyzer (TriStarII 3020, Mike, USA). The UV-vis absorbance was measured by a UV-vis spectrophotometer (TU1901, PRISTON, China).

3. Photocatalytic Experiment

The photocatalytic experiments were conducted in a glass reactor (300 mL) which was positioned at a fixed distance of 8 cm from the fluorescent lamp (65 W, 550 nm). In each experiment, the reaction system was composed of appropriate amount of catalysts and 200 mL Cr(VI)-containing solution. Solution pH was adjusted to 2.5 by HCl before reaction and the whole process was under magnetic stirring. The suspensions were kept in darkness for 30 min before 90 min irradiation to reach adsorption equilibrium onto the surface of catalyst. At 30 min intervals, a small aliquot of the suspensions was withdrawn by syringe and filtered with a Millipore filter (pore size of 0.45 μm). The instant Cr(VI) concentration was then determined according to the diphenylcarbazide spectrophotometric method (GB 7467-87). The removal efficiency was calculated by the difference between the initial and instant Cr(VI) concentration. After reaction, the total chromium concentration was also measured by a similar method (GB 7466-87) to figure out the Cr(III) concentration in water. Several batch experiments were conducted to study the effects of light irradiation, N-TiO_2 dosage, initial concentration Cr(VI), inorganic cations and glucose.

RESULTS AND DISCUSSION

1. Characterizations

1-1. TEM Analysis

Fig. 1 shows the TEM images of virgin TiO_2 (a) and N-TiO_2 (b).

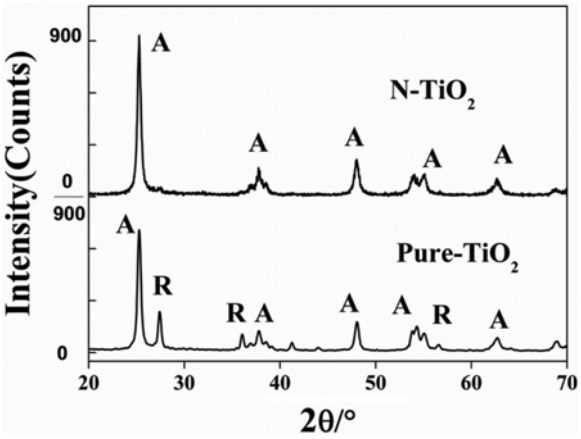

Fig. 2. XRD spectrum of virgin TiO_2 and N-TiO_2.

Compared with virgin TiO_2, N-TiO_2 particles not only have a higher dispersion but also have a smaller grain size of 25 nm, while the size of virgin TiO_2 is about 40 nm. It indicates N-doping has an inhibitory effect on the agglomeration and grain grow of TiO_2 particles. Thus, the quantum efficiency of N-TiO_2 was improved with respect to virgin TiO_2.

1-2. XRD Spectra Analysis

Fig. 2 shows the XRD spectra of virgin TiO_2 and N-TiO_2. There are both rutile peaks and anatase peaks seen in the spectra of virgin TiO_2, while N-TiO_2 is composed of pure anatase phase. The result shows the inhibitory effect of N-doping on the phase transformation of TiO_2. The result is probably owing to the presence of Ti-O-N bond, which is considered to inhibit the transformation from octahedral spiral chain of anatase to octahedral straight-chain of rutile [17]. Further, there is no new diffraction peak in N-TiO_2, suggesting that N atom did not change the crystalline structure of TiO_2 but successfully entered into the crystal lattice. The position of anatase phase (101) of virgin TiO_2 and N-TiO_2 were at 25.334°

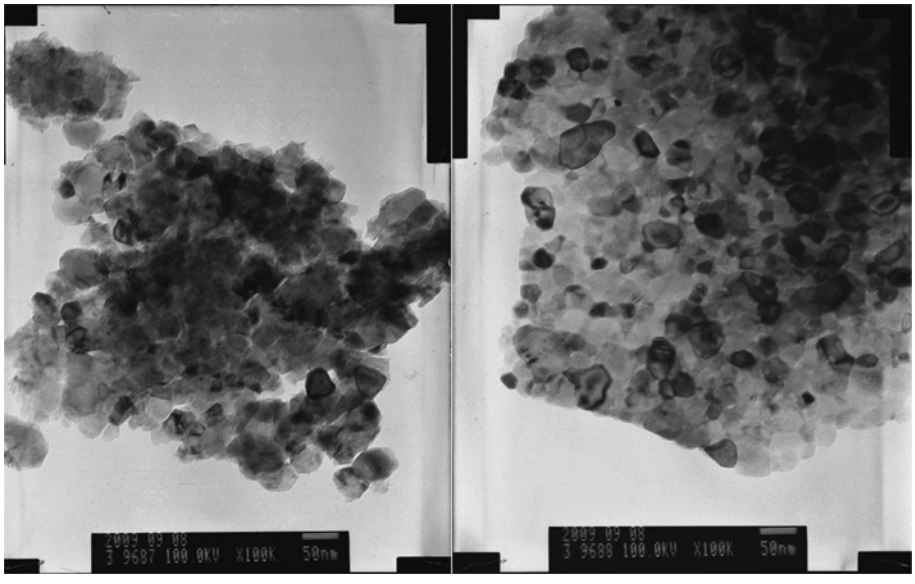

Fig. 1. TEM images of virgin TiO_2 (a) and N-TiO_2 (b).

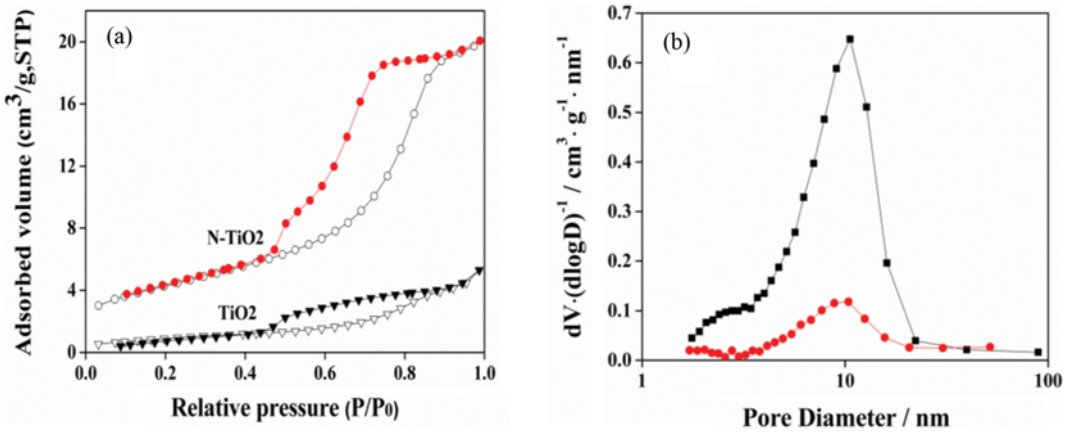

Fig. 3. The N_2 adsorption curves (a) and pore size distributions of virgin TiO_2 and N-TiO_2.

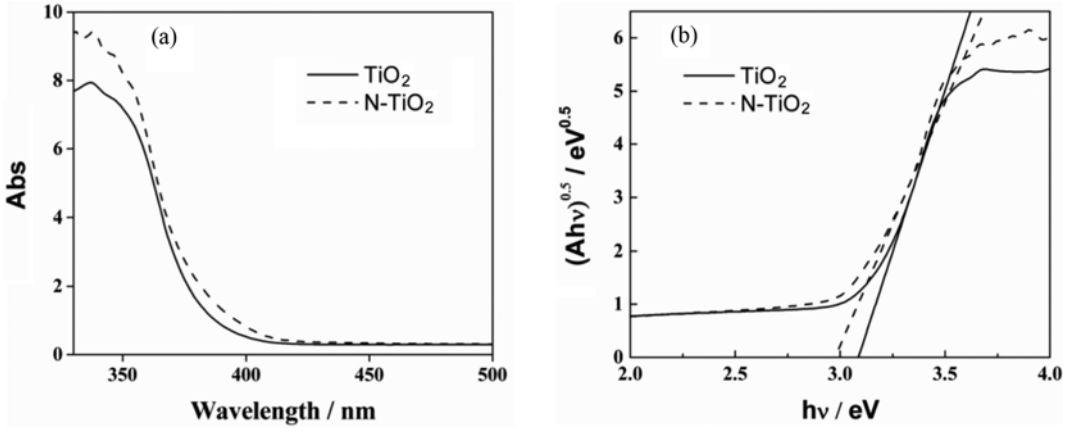

Fig. 4. UV-vis absorbance spectrum (a) and band gaps (b) of virgin TiO_2 and N-TiO_2.

and 25.246°, respectively, showing a left deviation after N-doping. The result indicates a larger interplanar distance according to Bragg's law, which also proves the substitution of O by N in the lattice.

Calculated by Scherrer formula, the particle sizes of virgin TiO_2 and N-TiO_2 are 29.8 nm and 19.9 nm, respectively (the lattice parameter is a little different from the commercially available catalysts or those prepared in other works cause of the different synthesis process). It suggests that N-doping has an inhibitory effect on the grain growth of TiO_2 particles, which is probably due to the deformation of crystal lattice and oxygen vacancies left by the substitution of O atoms by N atoms [18]. The decrease of particle size would shorten the time needed for photo-generated electrons moving to the surface of TiO_2, thus improving the quantum efficiency.

1-3. BET Analysis

Fig. 3 shows the N_2 adsorption-desorption isotherms (a) and the pore diameter distribution curves (b) of virgin TiO_2 and N-TiO_2. The curve of N-TiO_2 follows the IV adsorption isotherm on the basis of IUPAC classification, and the desorption curve of N-TiO_2 has greater distance from the adsorption curve. The result shows the better adsorption ability of N-TiO_2 than virgin TiO_2. As the desorption curve of TiO_2 is close to the adsorption curve, there are few pores on the surface. Further, as depicted in Fig. 3(b), N-doping helped form a uniform distribution of pore sizes which were mostly about 10 nm. The specific surface areas of N-TiO_2 and pure TiO_2 calculated according to the BJH model are 15.3 m^2/g and 3.4 m^2/g, respectively. Larger surface is advantageous to the adsorption of aqueous Cr(VI). The results show that the surface of TiO_2 was modified successfully.

1-4. UV-vis DRS Analysis

Fig. 4 shows the UV-vis DRS spectra of virgin TiO_2 and N-TiO_2 catalysts. After N-doping, there is an absorption spectra red-shift into the visible region. It is probably because N-insertion mixed the N 2p and O 2p states and narrowed the band gap of TiO_2, thus enabling the catalyst to absorb the light of larger wavelength [19].

To further study the optical properties, band-gap energies (Eg) for all these photocatalysts were calculated by making a plot of $(Ah\nu)^{1/2}$ versus hν in Fig. 4(b). The forbidden band widths of N-TiO_2 and TiO_2 are 2.98 eV and 3.08 eV, respectively. The results confirm the stronger light absorption of N-TiO_2 than pure TiO_2, which agrees to the results reported in [20].

2. Effects of Light on the Reduction of Cr(VI)

Fig. 5 shows the effects of light on the removal of aqueous Cr(VI). 1.0 g of N-TiO_2 was added into 200 mL of Cr(VI)-containing solutions (3 mg/L) as catalysts. There are two groups: the dark reaction means there was no light during the whole process, while the other group was the same as we mentioned in section 2.3. As depicted,

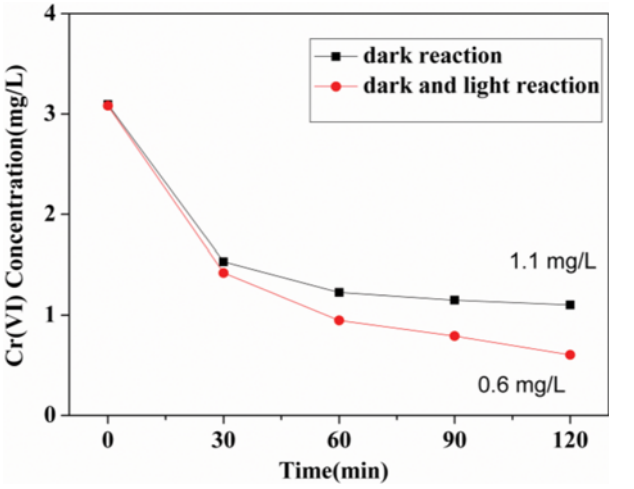

Fig. 5. The effects of light on the photoreduction of Cr(VI).

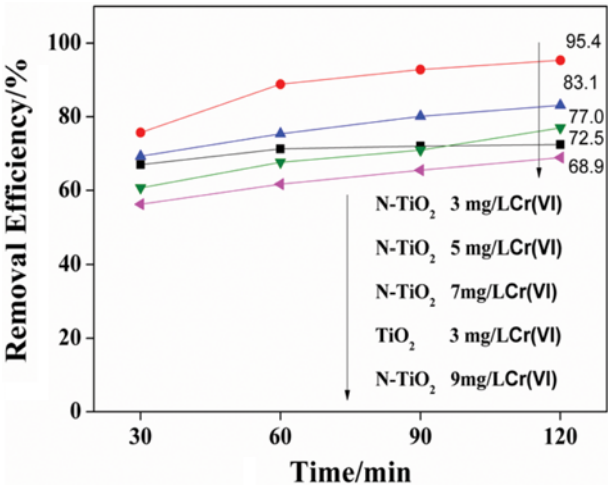

Fig. 7. The effects of initial concentration of Cr(VI) on the photoreduction of Cr(VI).

the catalyst almost reached the adsorption saturation after 30 min darkness. Further, there was an evident difference of Cr(VI) concentration between the two groups, especially after 120 min. At that time, the removal efficiency of the two groups reached 63.3% and 83.7%, respectively. The results suggested that the whole process involved adsorption at dark and photocatalytic reduction under visible light. During the photoreduction process, more than 20% of the removed Cr(VI) was further reduced by N-TiO_2 (the percentage was a little low as we did not include the Cr(III) ions adsorbed on the surface of N-TiO_2), indicating the visible light responding ability of N-TiO_2.

3. Effects of N-TiO_2 Dosage on the Reduction of Cr(VI)

Fig. 6 shows the effects of different N-TiO_2 dosage on the removal of aqueous Cr(VI). 0.5 g, 1.0 g, 1.5 g and 2.0 g of N-TiO_2 were added into 200 mL of Cr(VI)-containing solutions (3 mg/L), respectively. The removal efficiency was measured after 30 min darkness and 90 min light irradiation. As depicted, the efficiency increased evidently with the increase of catalyst dosage. However, when the amount of N-TiO_2 increased to 1.5 g, the efficiency reached 95% and entered a plateau. Therefore, 7.5 g/L is an economical optimum dosage. The reason could be that the number of photo-generated electrons increased with the increase of N-TiO_2 dosage. However, when the dosage exceeded a certain value, the catalyst would aggregate together, thus hindering the utilization of light.

4. Effects of Initial Concentration of Target Pollutant (in the Present Case Cr(VI)) on the Reduction of Cr(VI)

Fig. 7 shows the effects of different initial concentration of target pollutant (in the present case Cr(VI)) on the removal of aqueous Cr(VI). 1.5 g of N-TiO_2 was added into 200 mL of Cr(VI)-containing solutions (3 mg/L, 5 mg/L, 7 mg/L, 9 mg/L) as catalysts. Virgin TiO_2 was also used for comparison. As depicted, lower initial concentration of Cr(VI) was favorable to the degradation process and the removal efficiency using N-TiO_2 could reach 95.4% when the initial concentration was 3 mg/L. Further, the removal efficiency by N-TiO_2 was higher than that by TiO_2 both at 30 min and 120 min. The result suggests N-TiO_2 has better adsorption ability and photoactivity than TiO_2.

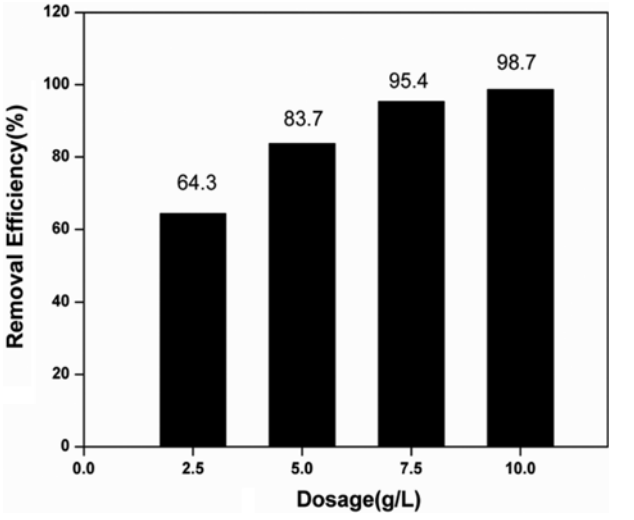

Fig. 6. The effects of N-TiO_2 dosage on the photoreduction of Cr(VI).

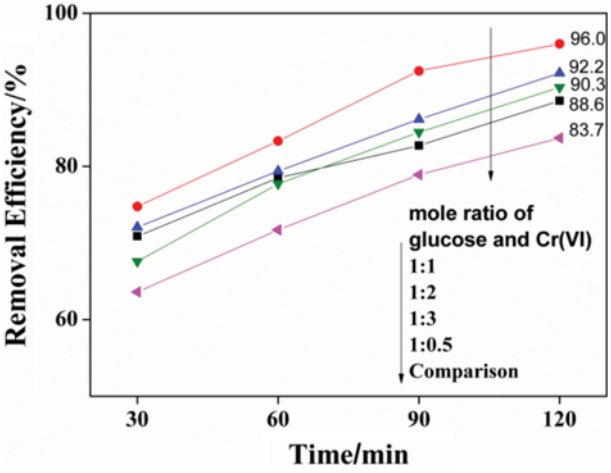

Fig. 8. The effects of glucose addition on the photoreduction of Cr(VI).

Table 1. Effect of inorganic cations on the reduction of Cr(VI)

Time	Mg^{2+}	Al^{3+}	Na^{+}	Control group
30 min	63.4%	61.6%	63.7%	63.6%
120 min	94.6%	92.4%	88.9%	85.6%

5. Effects of Glucose on the Reduction of Cr(VI)

To further understand the photocatalytic reduction process, we chose one kind of hole scavenger (in this case glucose) to study its effects on the reduction of Cr(VI). The results are shown in Fig. 8. 1.0 g of N-TiO_2 and different amount of glucose were added into 200 mL of Cr(VI)-containing solutions (3 mg/L) as catalysts. The experimental process was the same as mentioned in section 2.3. As depicted, the removal efficiency of Cr(VI) by N-TiO_2 reached the highest point (96.6%) when the mole ratio of glucose and Cr(VI) was 1 : 1, while the efficiency for the comparison group without glucose was only 83.7%. The result was due to the inhibitory effect of glucose on the recombination of electrons and holes. In this section, the photoreduction process was proved to exist and glucose was confirmed as a good promoter for Cr(VI) removal. However, too much glucose would compete with the adsorptive sites on the surface of N-TiO_2 with Cr(VI) and decrease the removal efficiency.

6. Effects of Inorganic Cations on the Reduction of Cr(VI)

As there are usually some inorganic cations coexisting with Cr(VI) in the wastewater, we chose three common metal ions with different chemical valence to study the effects of inorganic cations on the photoreduction of Cr(VI). The results are shown in Table 1. 1.0 g of N-TiO_2 and 0.2 mol of metal salts were added into 200 mL of Cr(VI)-containing solutions (3 mg/L) as catalysts. A control group without adding other cations is also presented for comparison. As shown, the removal efficiency of Cr(VI) increased in all groups, while there is some difference from group to group. The reason lies in two aspects. For Mg^{2+} and Al^{3+}, they both have strong ability of attracting electrons and transferring these electrons to Cr(VI) owing to the high charge states and small ionic radius. For Na^{+}, as it cannot play the same role, the possible reason may be related to Cl^{-} ions (it came from the added NaCl salt). It is suggested that Cl^{-} could capture •OH groups created from the reaction of water and photoinduced holes, thus promoting the photoreduction process [21]. The results prove that the interference of some inorganic cations could enhance the photocatalytic activity of N-TiO_2.

7. Kinetic Analysis

As the photoreduction process is reported to follow the pseudo-first kinetic model [22], we plotted a graph of $Ln(C_0/C_t)$ versus time in Fig. 9 to explore the kinetic mechanism. As shown, the experimental data basically matches the first-order kinetic model and the slopes of the lines equal the reaction rate constant. With the increase of initial Cr(VI) concentration, the reaction rate constant of N-TiO_2 groups varied from 0.0204 min^{-1} to 0.0025 min^{-1}, which were all larger than that of pure TiO_2 group (0.0010 min^{-1}). It suggests that the photoactivity was improved by N doping.

In the whole photocatalytic process, there are two major sections influencing the reaction rate: the mass transfer process and the catalytic reaction on the surface of catalyst [6]. If the diffusion of reactants was the rate control step, the reaction rate would rise

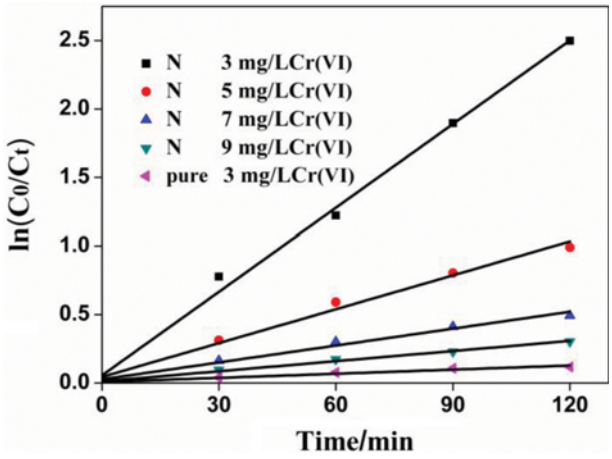

Fig. 9. First-order kinetic curves at different initial Cr(VI) concentration.

with the increase of initial Cr(VI) concentration. On contrary, if the catalytic reaction was the rate control step, the reaction rate would drop with the increase of initial Cr(VI) concentration. Therefore, we conclude that the photocatalytic reduction is the rate control step.

8. Photoreduction Process Analysis

The UV-vis absorption spectrum of different systems is shown in Fig. 10.

In Fig. 10(a), the absorbance of Cr(III) at the wavelength of 250-600 nm was almost zero, while Cr(VI) solutions had two absorption peaks at 260 nm and 350 nm. The mixture of Cr(III) and Cr(VI) had similar absorption peaks with Cr(VI) solutions.

In Fig. 10(b), Cr(VI) solutions of different concentrations had different absorbance at the same wavelength.

In Fig. 10(c), $K_2Cr_2O_7$ solutions and K_2CrO_4 solutions had two different absorption peaks at 250-600 nm. The absorption peaks of the mixture solution were at 269 nm and 370 nm closer to the peaks of K_2CrO_4.

In Fig. 10(d), the absorption peaks of the reaction system composed of K_2CrO_4 and catalysts were at 263 nm and 363 nm after 8.5 h light irradiation. Then the peaks moved to 266 nm and 366 nm after 23 h reaction. The results suggest that $Cr_2O_7^{2-}$ was gradually transformed to CrO_4^{2-} during the reaction. The process is suggested as the following:

$$Cr_2O_7^{2-} + H_2O \rightarrow 2HCrO_4^{-} \quad (1)$$

$$Cr_2O_7^{2-} + OH^{-} \rightarrow HCrO_4^{-} + CrO_4^{2-} \quad (2)$$

$$HCrO_4^{-} + OH^{-} \rightarrow CrO_4^{2-} + H_2O \quad (3)$$

H^{+} ions were consumed in the photoreduction of Cr(VI). Thus, pH increased and more $Cr_2O_7^{2-}$ transferred to CrO_4^{2-}. Since $Cr_2O_7^{2-}$ is more easily reduced than CrO_4^{2-} (the standard electrode potential of $Cr_2O_7^{2-}/Cr^{3+}$ and CrO_4^{2-}/Cr^{3+} is 1.33 V and 0.13 V, respectively), the pH value of the reaction system should be controlled in the photoreduction process. The result is consistent with the conclusion found in our previous work [16].

9. Mechanism Analysis

1.0 g of N-TiO_2 and virgin TiO_2 was, respectively, added into

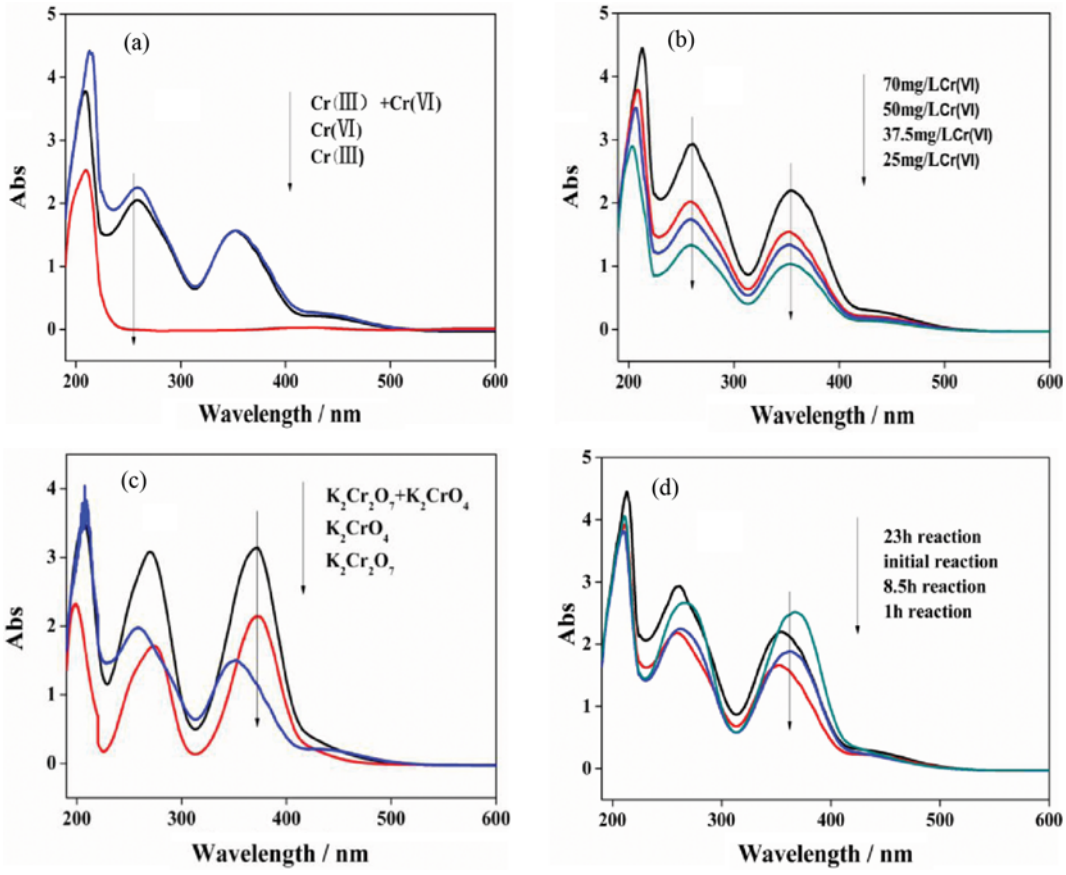

Fig. 10. UV-vis absorption spectrum of (a) Cr(VI) and Cr(III), (b) solutions of different Cr(VI) concentration, (c) solutions containing $K_2Cr_2O_7$ and K_2CrO_4 and (d) reaction systems at different time.

Cr(VI)-containing solutions (3 mg/L) to study the photoreduction mechanism. The experimental process was the same as mentioned in section 2.3. For N-TiO_2, after 120 min, the concentration of total chromium and Cr(VI) was 0.82 mg/L and 0.42 mg/L, respectively. It indicates that a certain amount of Cr(VI) was reduced to Cr(III). As for virgin TiO_2, the total chromium concentration was the same as the remaining Cr(VI) concentration, which shows that no Cr(VI) was reduced. The results suggest that N-doping enabled TiO_2 to respond to the visible light.

The photocatalytic process of Cr(VI) using N-TiO_2 involved two processes: adsorption and photocatalytic reduction. Cr(VI) was first adsorbed onto the surface of N-TiO_2 and then reduced to Cr(III) after getting the photo-generated electrons. Afterwards, residual Cr(VI) ions in water moved onto the surface and the reduction products Cr^{3+} and O_2 left the surface of N-TiO_2.

The reaction mechanism suggested was as the following:

$$\text{N-TiO}_2+h\nu\rightarrow e^-+h^+ \quad (4)$$

$$\text{Cr(VI)}\rightarrow \text{Cr(VI)}_{ads} \quad (5)$$

$$Ti^{4+}+e^-\rightarrow Ti^{3+} \quad (6)$$

$$3Ti^{3+}+\text{Cr(VI)}\rightarrow 3Ti^{4+}+Cr^{3+}{}_{ads} \quad (7)$$

$$\text{Cr(VI)}+3e^-\rightarrow Cr^{3+}{}_{ads} \quad (8)$$

$$Cr^{3+}{}_{ads}\rightarrow Cr^{3+} \quad (9)$$

$$H_2O+h^+\rightarrow H^++\bullet OH \quad (10)$$

$$2\bullet OH\rightarrow H_2O+1/2\ O_2 \quad (11)$$

CONCLUSIONS

N-TiO_2 with enhanced photoactivity was prepared via sol-gel method. It was characterized by TEM, XRD, BET and UV-vis DRS techniques. From TEM, N-TiO_2 has smaller grain size than virgin TiO_2. XRD proves the inhibitory effect of N-doping on the phase transformation and grain growth of TiO_2. In BET analysis, better adsorption ability was obtained by N-doping. UV-vis DRS spectrum indicates N-doping successfully narrowed the band gap and improved the absorption of visible light.

In the photocatalytic experiments, five factors were studied for their effects on the removal efficiency of aqueous Cr(VI). The whole reaction can be divided into adsorption and photoreduction. Light irradiation is essential to the second process and only N-TiO_2 can respond to visible light. The removal efficiency increased with the increase of catalyst dosage or the decrease of initial Cr(VI) concentration. Further, adding an appropriate amount of glucose can promote the photocatalytic process owing to its ability of capturing excess photoinduced holes. Several inorganic ions like Mg^{2+}, Al^{3+} and Cl^- were also proved to be able to improve the quantum efficiency. The photocatalytic reaction was confirmed as the rate

control step in kinetic analysis.

ACKNOWLEDGEMENTS

This work was financially supported by Natural Science Foundation of Hebei (No. E2014502111) and National Natural Science Foundation of China (No. 51476056).

REFERENCES

1. X. Y. Zhang, H. S. Chen and D. N. Fang, *J. Solid State Electrochem.*, **20**(10), 2835 (2016).
2. Y. H. Bao, X. Y. Zhang, X. Zhang, L. Yang, X. Y. Zhang, H. S. Chen, M. Yang and D. N. Fang, *J. Power Sources*, **321**, 120 (2016).
3. X. Y. Zhang, L Yang, F. Hao, H. S. Chen, M. Yang and D. N. Fang, *Nanomaterials*, **5**(4), 1985 (2015).
4. X. Y. Zhang, F. Hao, H. S. Chen and D. N. Fang, *Mechanics Mater.*, **91**, 351 (2015).
5. A. E. Giannakas, E. Seristatidou, Y. Deligiannakis and I. Konstantinou, *Appl. Catal. B: Environ.*, **132-133**, 460 (2013).
6. H. J. Wang, X. J. Wu, Y. L. Wang, Z. B. Jiao, S. W. Yan and L. H. Huang, *Chinese J. Catal.*, **32**(4), 637 (2011).
7. V. Pifferi, F. Spadavecchia and G. Cappelletti, *Catal. Today*, **209**, 8 (2013).
8. Q. Sun, H. Li, S. L. Zheng and Z. M. Sun, *Appl. Surf. Sci.*, **311**, 369 (2014).
9. W. Liu, J. R. Ni and X. C. Yin, *Water Res.*, **53**, 12 (2014).
10. Z. M. Sun, L. M. Zheng, S. L. Zheng and Ray L. Frost, *Colloid Interface Sci.*, **404**, 102 (2013).
11. H. R. Zheng, Y. J. Cui and J. S. Zhang, *Chinese J. Catal.*, **32**(1), 100 (2011).
12. H. J. Yun, D. M. Lee, S. Yu, J Yoon, H. J. Park and J. Yi, *J. Mol. Catal. A Chem.*, **378**(11), 221 (2013).
13. S. Z Hu, A. J. Wang, X. Li and Holger Löwe, *J. Phys. Chem. Solids*, **71**, 156 (2010).
14. M. Z. Xie, Y. J. Feng, P. Luan, J. Bian and L. Q. Jing, *Chinese J. Inorg. Chem.*, **30**(9), 2081 (2014).
15. K. Cendrowski, M. Jedrzejczak, M. Peruzynska, A. Dybusb, M. Drozdzik and Ewa Mijowska, *Alloys Comp.*, **605**, 173 (2014).
16. S. Q. Wang and D. L. Zhang, *Adv. Mater. Res.*, **610-613**, 1497 (2013).
17. X. Y. Chen, D. H. Kuo and D. F Lu, *Chem. Eng. J.*, **295**, 192 (2016).
18. K. Zhang, X. D. Wang, T. O. He, X. L. Guo and Y. M. Feng, *Powder Technol.*, **253**, 608 (2014).
19. N. T. Nolan, D. W. Synnott, M. K. Seery, S. J. Hinder, A. V. Wassenhoven and S. C. Pillai, *Hazard. Mater.*, **211**, 88 (2012).
20. A.-A. Salarian, Z. Hami, N. Mirzaei, S. M. Mohseni, A. Asadi, H. Bahrami, M. Vosoughi, A. Alinejad and M. R. Zare, *J. Mol. Liq.*, **220**, 183 (2016).
21. X. C. Ren, G. Z. Chang, Y. M. Zhu, H. F. Liu and M. Cao, *Environ. Chem.*, **28**(06), 288 (2009).
22. A. Peter, L. Mihaly-Cozmuta, A. M. Cozmuta, N. Camelia, L. B. Tudoran and L. Baia, *Mater. Technol.*, **29**(3), 129 (2014).